AMERICAN SOCIETY FOR MICROBIOLOGY | Applied and Environmental Microbiology®

ENZYMOLOGY AND PROTEIN ENGINEERING

A New Group of Modular Xylanases in Glycoside Hydrolase Family 8 from Marine Bacteria

Xiu-Lan Chen,[a] Fang Zhao,[a] Yong-Sheng Yue,[a] Xi-Ying Zhang,[a] Yu-Zhong Zhang,[a,b,c] Ping-Yi Li[a]

[a]State Key Laboratory of Microbial Technology, Institute of Marine Science and Technology, Marine Biotechnology Research Center, Shandong University, Jinan, China

[b]Laboratory for Marine Biology and Biotechnology, Qingdao National Laboratory for Marine Science and Technology, Qingdao, China

[c]College of Marine Life Sciences, Ocean University of China, Qingdao, China

ABSTRACT Xylanases play a crucial role in the degradation of xylan in both terrestrial and marine environments. The endoxylanase XynB from the marine bacterium *Glaciecola mesophila* KMM 241 is a modular enzyme comprising a long N-terminal domain (NTD) (E44 to T562) with xylan-binding ability and a catalytic domain (CD) (T563 to E912) of glycoside hydrolase family 8 (GH8). In this study, the long NTD is confirmed to contain three different functional regions, which are NTD1 (E44 to D136), NTD2 (Y137 to A193), and NTD3 (L194 to T562). NTD1, mainly composed of eight β-strands, functions as a new type of carbohydrate-binding module (CBM), which has xylan-binding ability but no sequence similarity to any known CBM. NTD2, mainly forming two α-helices, contains one of the α-helices of the catalytic domain's $(\alpha/\alpha)_6$ barrel and therefore is essential for the activity of XynB, although it is far away from the catalytic domain in sequence. NTD3, next to the catalytic domain in sequence, is shown to be helpful in maintaining the thermostability of XynB. Thus, XynB represents a kind of xylanase with a new domain architecture. There are four other predicted glycoside hydrolase sequences with the same domain architecture and high sequence identity ($\geq$80%) with XynB, all of which are from marine bacteria. Phylogenetic analysis shows that XynB and these homologs form a new group in GH8, representing a new class of marine bacterial xylanases. Our results shed light on xylanases, especially marine xylanases.

IMPORTANCE Xylanases play a crucial role in natural xylan degradation and have been extensively used in industries such as food processing, animal feed, and kraft pulp biobleaching. Some marine bacteria have been found to secrete xylanases. Characterization of novel xylanases from marine bacteria has significance for both the clarification of xylan degradation mechanisms in the sea and the development of new enzymes for industrial application. With *G. mesophila* XynB as a representative, this study reveals a new group of the GH8 xylanases from marine bacteria, which have a distinct domain architecture and contain a novel carbohydrate-binding module. Thus, this study offers new knowledge on marine xylanases.

KEYWORDS modular xylanase, glycoside hydrolase family 8, N-terminal domain, carbohydrate-binding module, catalysis

Xylan, a major component of plant hemicellulose, is a complex, highly branched heteropolymer. Endo-β-1,4-xylanases (EC 3.2.1.8) are glycosidases that cleave the internal β-1,4-xylosidic bonds of the main chain of xylan and produce unbranched or branched xylooligosaccharides (1). Due to the complexity of the xylan structure, endo-β-1,4-xylanases are diverse in sequences, structures, hydrolytic activities, and enzymatic properties. They are distributed in glycoside hydrolase (GH) families 5, 7, 8,

Received 22 July 2018 **Accepted** 12 September 2018

Accepted manuscript posted online 14 September 2018

Citation Chen X-L, Zhao F, Yue Y-S, Zhang X-Y, Zhang Y-Z, Li P-Y. 2018. A new group of modular xylanases in glycoside hydrolase family 8 from marine bacteria. Appl Environ Microbiol 84:e01785-18. https://doi.org/10.1128/AEM.01785-18.

Editor Claire Vieille, Michigan State University

Copyright © 2018 American Society for Microbiology. All Rights Reserved.

Address correspondence to Ping-Yi Li, lipingyipeace@sdu.edu.cn.

X.-L.C. and F.Z. contributed equally to this work.

10, 11, and 43. Among endo-β-1,4-xylanases, those from GH family 10 (GH10) and GH11 have been studied in more detail. GH10 xylanases have an $(\alpha/\beta)_8$ barrel structure (2), while GH11 xylanases have a β-jelly roll structure (3). Despite their different structures, both enzyme families adopt the catalytic mechanism of anomeric retention to release xylooligosaccharides from xylan (2, 3).

The endo-β-1,4-xylanases in GH family 8 reported so far include XylY from *Bacillus* sp. strain KK-1 (4), PhXyl from *Pseudoalteromonas haloplanktis* (5), Xyn8 from *Pseudoalteromonas arctica* (6), rXyn8 from an uncultured bacterium (7, 8), XYL6806 from uncultured insect gut microbes (9), Xyn8A from the human gut microbe *Bacteroides intestinalis* DSM 17393 (10), and XynB from *Glaciecola mesophila* KMM 241 (11). Except for XYL6806 and XynB, the other GH8 xylanases are all single-domain enzymes containing only a catalytic domain (CD). Among these xylanases, only the crystal structure of PhXyl (PDB accession number 1H13) has been solved. PhXyl adopts an $(\alpha/\alpha)_6$ barrel fold, different from the structures of GH10 and GH11 xylanases (12). Moreover, the GH8 endoxylanases cleave xylan by an anomeric inversion mechanism. Structural and mutational analyses indicate that residues E78, D281, Y203, and D144 play essential roles in PhXyl (13). E78 functions as the general acid, D281 functions as the general base, Y203 helps in maintaining the position of the nucleophilic water molecule and in structural integrity, and D144 plays an essential role in sugar ring distortion and transition-state stabilization (13). These GH8 xylanases are strict endoxylanases with different profiles for the hydrolysis products. XynB, XYL6806, and PhXyl function in a similar way, efficiently hydrolyzing xylohexaose and xylan into xylobiose, xylotriose, and xylotetraose (5, 9, 11). Xyn8 functions in a different way, selectively releasing xylotriose from substrates (8). In addition, several reducing-end xylose-releasing exo-oligoxylanases (EC 3.2.1.156) belonging to GH family 8 have also been reported (14, 15).

XYL6806 and XynB are two reported modular endo-β-1,4-xylanases in GH family 8. XYL6806 contains 1,395 amino acid residues and is composed of an N-terminal domain (NTD) of unknown function (residues M1 to P638), a catalytic domain of GH family 8 (residues T650 to M1050), and a C-terminal carbohydrate-binding module (CBM) of family 3 (residues A1100 to K1395) (9). XynB contains 912 amino acid residues and is composed of a signal peptide (residues M1 to A43), an NTD (residues E44 to R584), and a GH8 catalytic domain (residues S585 to E912) (11). Thus, XYL6806 and XynB are two GH8 xylanases with different domain architectures. The NTD of XynB, which contains 541 residues, has been shown to have the ability to bind insoluble xylan (11). This suggests that the NTD likely contains one or more CBMs. However, because the NTD of XynB has no obvious similarity to any CBM sequence in public databases, the CBM(s) in the NTD has not been predicted or identified. Moreover, whether the NTD of XynB contains another functional region(s) is also unknown.

In this study, to identify the CBM in the NTD of XynB, we investigated the functions of different regions of the long NTD of XynB through sequence analysis and truncation mutagenesis. We found that the NTD contains three different functional regions. NTD1, containing residues E44 to D136, is a novel CBM that has xylan-binding ability but no sequence similarity to any known CBM. NTD2, containing residues Y137 to A193, forms two α-helices and is a structural element of the $(\alpha/\alpha)_6$ barrel fold of the catalytic domain. NTD3, containing residues L194 to T562, is helpful in maintaining the thermostability of XynB. Moreover, phylogenetic analysis indicates that XynB and its homologs, which are all from marine bacteria, represent a new group of the GH8 xylanases. Our results show that XynB and its homologs are a class of marine bacterial xylanases with a new domain architecture.

RESULTS

Sequence analysis and subdivision of the N-terminal domain of XynB. A previous study showed that the NTD of XynB had xylan-binding ability (11). To identify the possible CBM in the NTD and the other possible function(s) of the NTD, multiple-sequence alignment and secondary structure prediction of XynB were performed. Until now, only two GH8 xylanases with structures have been reported, the endoxylanase

PhXyl (12) and the reducing-end xylose-releasing exo-oligoxylanase BhRex from *Bacillus halodurans* (15, 16). Both PhXyl and BhRex adopt an $(\alpha/\alpha)_6$ barrel fold. Sequence analysis indicated that the catalytic domain of XynB shares high similarity with full-length PhXyl and BhRex, excluding their N-terminal α-helices α1 to α3 and β-strands β1 to β3, and that the large NTD of XynB shares no similarity with PhXyl and BhRex, except for residues Y137 to A193 and T563 to R584 (Fig. 1). Surprisingly, residues Y137 to A193 in the NTD of XynB share significant similarity with the N-terminal α-helices α1 to α3 of PhXyl and BhRex (Fig. 1). For both PhXyl and BhRex, α3 is an essential structural element of their $(\alpha/\alpha)_6$ barrels (12, 16). Psipred prediction also suggested that residues Y137 to A193 in the NTD of XynB likely form two α-helices (see Fig. S1 in the supplemental material). These analyses imply that it is likely that residues Y137 to A193 in the NTD of XynB form α-helices and are a structural element of the catalytic domain. In addition, because the sequence spanning residues T563 to R584 of XynB has significant similarity with the corresponding sequences in PhXyl and BhRex (Fig. 1), T563 to R584 should be a part of the catalytic domain of XynB, rather than a part of the NTD as stated in a previous study (11). Based on these analyses, the NTD (residues E44 to T562) and the catalytic domain (residues T563 to E912) of XynB were redefined, and the NTD was divided into three regions, NTD1 (residues E44 to D136), NTD2 (residues Y137 to A193), and NTD3 (residues L194 to T562) (Fig. 2). The functions of these regions of NTD were further investigated.

NTD1 functions as a CBM. A previous study found that the recombinant NTD of XynB showed the ability to bind strongly to insoluble xylan and Avicel (11). To reveal which region in the NTD of XynB functions as a CBM, the abilities of recombinant NTD1 and NTD2-NTD3 to bind to insoluble beechwood xylan were examined and compared to that of the NTD (Fig. 3). NTD1 showed xylan-binding ability similar to that of the NTD, whereas NTD2-NTD3 showed little xylan-binding ability, suggesting that in the NTD of XynB, only the NTD1 region functions as a CBM. To compare the xylan-binding abilities of wild-type (WT) XynB and its NTD1 deletion mutant XynBΔNTD1, two inactive mutants, XynB(D646A) and XynB(D646A) ΔNTD1, were constructed in order to avoid the hydrolysis of xylan during analysis of xylan binding. The XynB(D646A) ΔNTD1 mutant had xylan-binding ability, which was slightly weaker than that of XynB(D646A), suggesting that both NTD1 and the catalytic domain, which has a substrate-binding pocket, can bind insoluble xylan. However, the K_m value for XynBΔNTD1 toward soluble arabinoxylan was only a little higher than that of WT XynB (Table 1; see also Fig. S2 in the supplemental material), and XynBΔNTD1 showed a specific activity similar to that of WT XynB toward insoluble xylan and a much higher specific activity toward soluble xylan (Fig. 2). Therefore, it seems that NTD1 is not essential for XynB in xylan hydrolysis, although it has xylan-binding ability.

CBMs are usually small domains composed of mainly β-strands (17). Secondary structure prediction showed that the small NTD1 contains eight putative β-strands (Fig. S1), which further supports the conclusion that NTD1 functions as a CBM. According to amino acid sequence similarities, CBMs are now classified into 81 families in the CAZy database (18). BLAST analysis indicated that NTD1 shows no obvious similarity to any known CBM in sequence, suggesting that the NTD1 segment of XynB represents a new type of CBM.

NTD2 is a component of the catalytic domain. For many modular glycoside hydrolases, the separately expressed catalytic domain shows glycoside hydrolase activity (19–21). However, the separately expressed CD (T563 to E912) of XynB was completely inactive (Fig. 2), implying that another region(s) in the NTD of XynB might be essential for enzyme activity. As described above, sequence analysis indicated that NTD2 is possibly a component of the catalytic domain of XynB (Fig. 1 and Fig. S1). To confirm this, we investigated whether NTD2 is necessary for the activity of XynB by comparing the activities of mutants XynBΔNTD1 (Y137 to E912, lacking only NTD1), NTD2-CD (Y137 to A193/T563 to E912, lacking both NTD1 and NTD3), and NTD3-CD (L194 to E912, lacking both NTD1 and NTD2). Mutant NTD3-CD was inactive toward

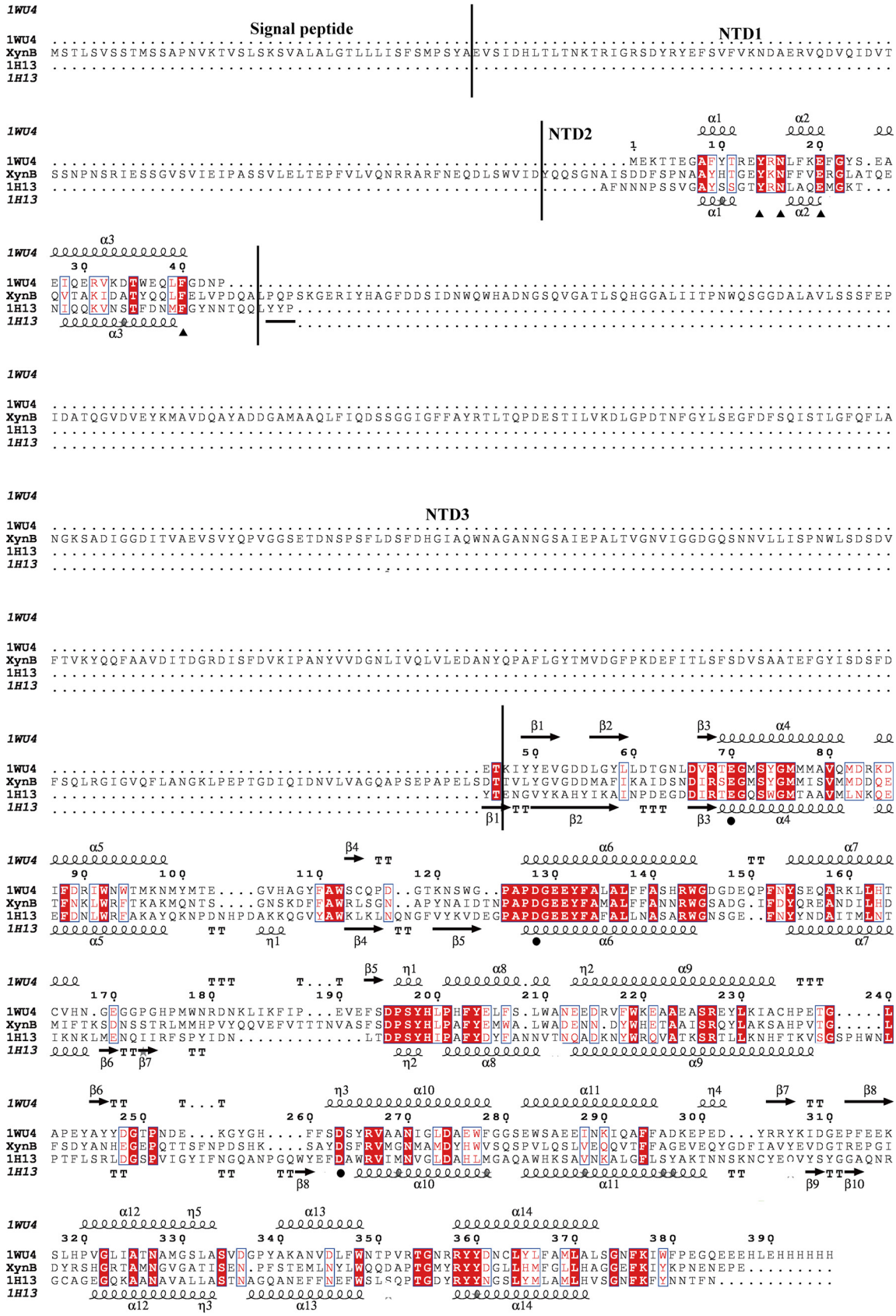

FIG 1 Alignment of the sequences of XynB and two other reported GH8 xylanases. The two reported GH8 xylanases are the endoxylanase PhXyl from *Pseudoalteromonas haloplanktis* (PDB accession number 1H13) and the reducing-end xylose-releasing

(Continued on next page)

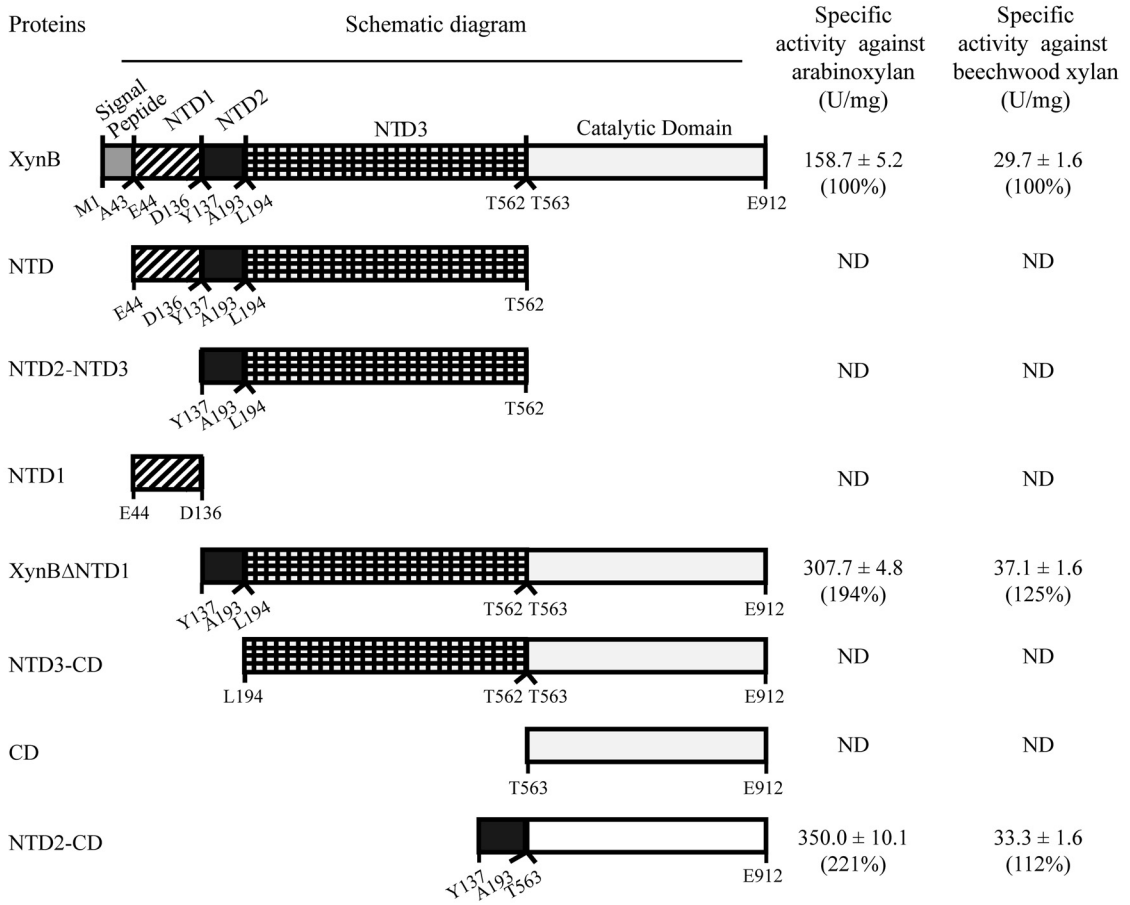

FIG 2 Schematic diagram of the domain architecture of XynB and its mutants. The specific activities of XynB and its mutants toward 30 mg/ml arabinoxylan or beechwood xylan were determined at 40°C and pH 7.0. The data shown in the graph are from triplicate experiments (means ± standard deviations [SD]). ND indicates that enzyme activity was not detectable.

beechwood xylan and arabinoxylan, whereas mutants XynBΔNTD1 and NTD2-CD were active (Fig. 2), indicating that NTD2 is essential for the activity of XynB. Therefore, sequence analysis in combination with mutational and biochemical analyses suggest that mutant NTD2-CD is the true catalytic domain of XynB.

To further confirm that NTD2-CD is the true catalytic domain of XynB, we modeled the structure of NTD2-CD. Among all the xylanases with structures, mutant NTD2-CD shows the most significant sequence identity to the single-domain enzymes BhRex (36%) (16) and PhXyl (31%) (12) over the length of these enzymes. By using the structure of BhRex or PhXyl as the template, we modeled the structure of mutant NTD2-CD of XynB (Fig. 4). No matter which template was used, the modeled structure of mutant NTD2-CD has the $(\alpha/\alpha)_6$ fold, and the NTD2 region contains an α-helix that is an essential structural element of the $(\alpha/\alpha)_6$ barrel. In this model, NTD2 is far away from the substrate-binding pocket of mutant NTD2-CD (Fig. 4A). This is supported by site-directed mutational analysis of conserved residues (Y159, N161, E165, and F186) in NTD2 of XynBΔNTD1 (Fig. 1 and 4). Replacement of these residues by alanine caused

FIG 1 Legend (Continued)

exo-oligoxylanase BhRex from *Bacillus halodurans* (PDB accession number 1WU4). PhXyl and BhRex are both single-domain enzymes containing only a catalytic domain. Using ESPript, secondary structures of BhRex are shown above the alignment, and secondary structures of PhXyl are shown below the alignment. Helices are indicated by springs, strands are indicated by arrows, turns are indicated by TT, and 3_{10}-helices are indicated by η. Identical residues are shown in white on a red background, and similar residues are shown in bold red. Solid circles indicate residues (E586, D646, and D786) crucial for the catalytic activity of GH8 xylanases. Solid triangles indicate selected conserved residues (Y159, N161, E165, and F186) in NTD2 of XynB. The different regions in the NTD of XynB are also shown.

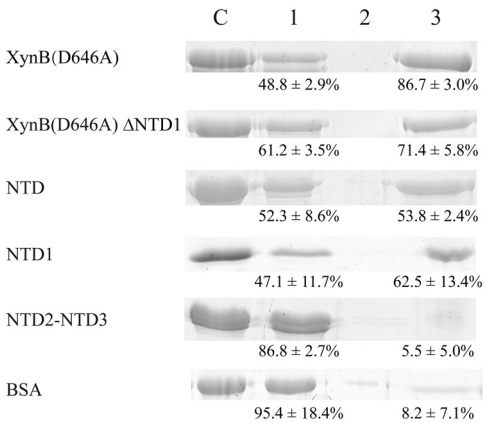

FIG 3 SDS-PAGE analysis of the abilities of WT XynB and its mutants to bind to insoluble beechwood xylan. Bovine serum albumin (BSA) (0.1 mg) was used as a negative control. Lane C, total proteins (control); lane 1, unbound proteins; lane 2, proteins in the wash buffer; lane 3, bound proteins. The percentages at the bottom of the gel are the densitometric ratios of each band compared with that of the control band, which are means ± SD of data from triplicate experiments. The data shown are representative of results of triplicate experiments.

no or a small impact on the K_m of XynBΔNTD1 (Table 1 and Fig. S2). Circular dichroism spectral analysis showed that these mutations caused no visible changes in the secondary structures of XynBΔNTD1 (Fig. S3).

Functional analysis of NTD3. To reveal the function of the NTD3 region, the biochemical properties of mutants XynBΔNTD1 and NTD2-CD, which lacks NTD3 compared to XynBΔNTD1, were studied and compared to those of WT XynB. Compared to XynBΔNTD1, NTD2-CD had a similar specific activity toward beechwood xylan or arabinoxylan (Fig. 2). This implies that NTD3 contributes little to the hydrolysis of XynB on the tested xylans. Next, with arabinoxylan as the substrate, we determined the effects of temperature, pH, and NaCl on the activities and stabilities of WT XynB, XynBΔNTD1, and NTD2-CD. NTD2-CD had the same optimal temperature (40°C) as WT XynB and XynBΔNTD1 but higher relative activity at temperatures below 40°C and lower thermostability at 35°C (Fig. 5A and B). This indicates that NTD3 is helpful in maintaining the thermostability of XynB but does not facilitate its cold adaptation. Compared with XynB and XynBΔNTD1, NTD2-CD showed high activity and high stability in 0 to 4 M NaCl (Fig. 5C and D), indicating that NTD2-CD has higher NaCl tolerance. There was little difference in the effects of pH on the activities and stabilities of XynB, XynBΔNTD1, and NTD2-CD. The three proteins all showed maximum activity at pH 7.0 and were stable in the range of pH 6.0 to 10.0 (Fig. 5E). Taken together, these mutational and biochemical results suggest that NTD3 increases the thermostability of XynB but does not contribute to its salt tolerance or cold adaptation.

TABLE 1 Kinetic parameters of recombinant XynB and its mutants for arabinoxylan[a]

Enzyme	Mean K_m (mg/ml) ± SD	Mean V_{max} (μmol/min/mg) ± SD	k_{cat} (s^{-1})	k_{cat}/K_m (s^{-1} mg/ml^{-1})
XynB	4.4 ± 0.3	173.4 ± 6.6	277.9	63.2
XynBΔNTD1	5.2 ± 0.3	332.0 ± 8.8	473.3	91.0
XynB(Y159A) ΔNTD1	4.3 ± 0.3	308.4 ± 9.6	439.7	102.1
XynB(N161A) ΔNTD1	4.3 ± 0.4	290.2 ± 13.2	413.7	96.2
XynB(E165A) ΔNTD1	5.4 ± 0.5	398.5 ± 19.7	568.1	105.2
XynB(F186A) ΔNTD1	3.2 ± 0.3	36.0 ± 1.4	51.3	16.0

[a]Kinetic parameters were calculated by nonlinear regression fit directly to the Michaelis-Menten equation. The initial rates were determined with 0 to 30.0 mg/ml arabinoxylan at 40°C. XynB(Y159A) ΔNTD1, XynB(N161A) ΔNTD1, XynB(E165A) ΔNTD1, and XynB(F186A) ΔNTD1 mutations were introduced into NTD2 of mutant XynBΔNTD1. Nonlinear fit curves for the hydrolysis of arabinoxylan by XynB and its mutants are shown in Fig. S2 in the supplemental material.

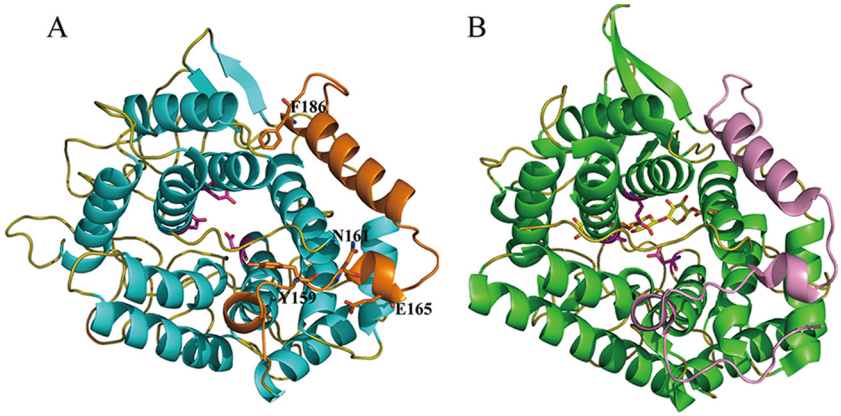

FIG 4 Structural model of mutant NTD2-CD. (A) Modeled structure of mutant NTD2-CD. The structure was modeled using the structure of the endoxylanase PhXyl (PDB accession number 1H13) as the template. NTD2 is shown in orange, and the catalytic domain is shown in cyan. Catalytic residues E586, D646, and D786 of XynB are shown as magenta sticks. Conserved residues Y159, N161, E165, and F186 in NTD2 are also shown. (B) Crystal structure of the D144A mutant of PhXyl in complex with xylopentaose (PDB accession number 2B4F). PhXyl is a single-domain enzyme containing only a catalytic domain. The region in PhXyl sharing similarity to NTD2 of XynB is shown in pink, and the other region is shown in green. Catalytic residues E78, D144 (replaced by Ala in the D144A mutant), and D281 are shown as magenta sticks, and xylopentaose is shown as yellow sticks.

XynB and its homologs form a new group of GH8 xylanases. Among the reported GH8 xylanases, XynB is most closely related to the single-domain endoxylanase rXyn8 (7, 8), with a low sequence identity of 39%, covering only 41% of the XynB sequence, suggesting that XynB is a new member of the GH8 xylanases. A similarity search against the NCBI nonredundant (nr) protein database revealed that there are four predicted glycoside hydrolase sequences sharing high identity (≥80%) with full-length XynB. Multiple-sequence alignment showed that these enzymes have the same domain architecture as XynB and that the key residues involved in the catalysis of XynB are conserved in these enzymes (see Fig. S4 in the supplemental material), suggesting that these glycoside hydrolases are xylanases that are similar to XynB. Phylogenetic analysis of the GH8 xylanases shows that XynB and its homologs are clustered as a group separate from the cluster of the reported GH8 xylanases (Fig. 6). XynB and its homologs are more closely related to endoxylanases than to exo-oligoxylanases in the phylogenetic tree. Therefore, based on sequence and phylogenetic analyses, XynB and its homologs represent a new group of GH8 xylanases. Interestingly, XynB and its homologs are all from marine bacteria, including the genera *Paraglaciecola* and *Pseudoalteromonas* (Fig. 6). This indicates that there is a class of bacterial xylanases from the sea with the same domain architecture as XynB.

DISCUSSION

Modular glycoside hydrolases usually contain one or more CBMs, which are known to facilitate the access of enzymes to insoluble polysaccharides and promote polysaccharides degradation (22). Until now, CBMs have been classified into 81 families based on amino acid sequence similarity in the CAZy database (18). The so-far-reported CBMs that modular endoxylanases contain are from different families, such as families 3, 4, 6, 8, 9, 13, 22, and 35 (9, 20, 21, 23–25). Our results in this study indicate that the modular GH8 xylanase XynB contains a CBM at its N terminus, which is composed of 93 residues (E44 to D136). Because this CBM has no obvious sequence similarity to any CBM in databases, it may represent a new type of CBM. The dominant folds among reported CBMs are β-sandwich and β-trefoil folds composed of mainly β-strands (17). Based on secondary structure prediction, the CBM in XynB is also composed mainly of β-strands. However, due to the lack of a crystal structure, the fold that the CBM in XynB adopts

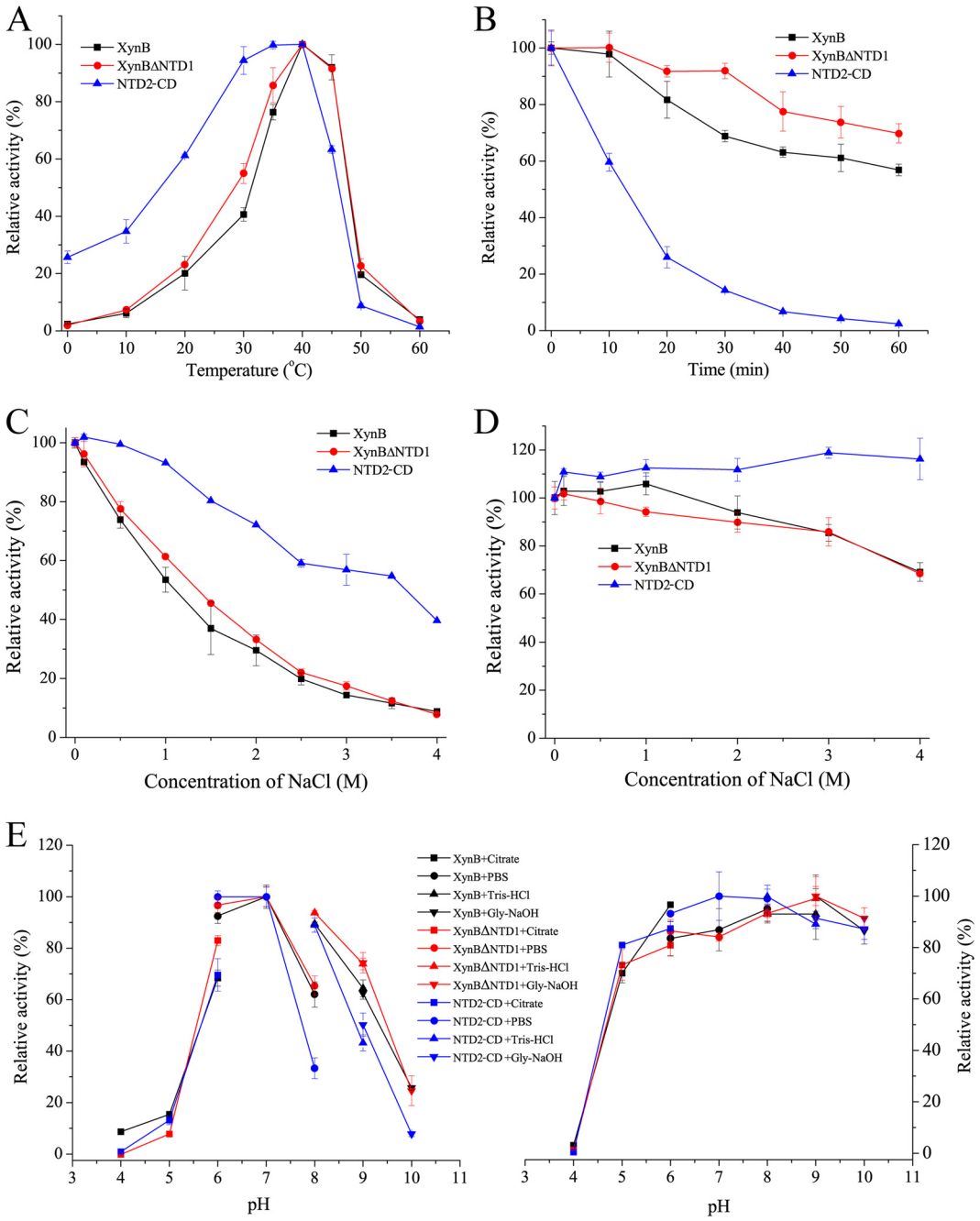

FIG 5 Effects of temperature, NaCl, and pH on the activities and stabilities of WT XynB and its mutants. (A) Effect of temperature on the activities of WT XynB and its mutants. (B) Effect of temperature on the stabilities of WT XynB and its mutants. The enzyme was incubated at 35°C for different periods. Residual activity was measured under optimal conditions. (C) Effect of NaCl on the activities of WT XynB and its mutants. (D) Effect of NaCl on the stabilities of WT XynB and its mutants. The enzyme was incubated in buffers containing different concentrations of NaCl (0 to 4 M) at 4°C for 1 h. Residual activity was measured under optimal conditions. (E) Effects of pH on the activities (left) and stabilities (right) of WT XynB and its mutants. To determine the effect of pH on enzyme stability, the enzymes were incubated at 4°C for 1 h in buffers ranging from pH 4.0 to 10.0. Residual activity was measured under optimal conditions. The activities of WT XynB, XynBΔNTD1, and NTD2-CD at 40°C (A), at 0 min (B), and with 0 M NaCl (C and D) and the maximum activities (E) were taken as 100%, respectively. The graphs show data from triplicate experiments (means ± SD).

and the key residues in this CBM involved in the binding of carbohydrate substrates are still unknown and need further study. In addition, the CBM does not seem to be essential for XynB in the hydrolysis of the tested xylan substrates, because XynBΔNTD1 shows a K_m similar to that of the full-length enzyme on soluble arabinoxylan, and the

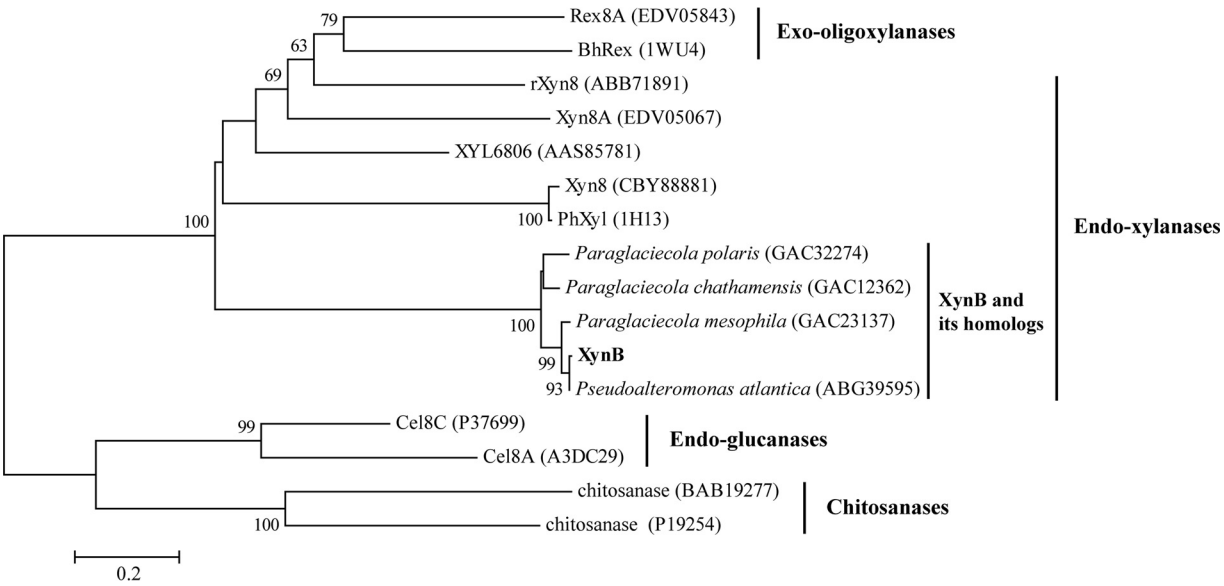

FIG 6 Phylogenetic tree of XynB and reported GH8 xylanases. The tree was built by using the neighbor-joining method with a Jones-Taylor-Thornton (JTT) matrix-based model using 297 amino acid positions. Bootstrap analysis of 1,000 replicates was conducted, and values above 50% are shown. The scale for the branch length is shown below the tree. Endoglucanases and chitosanases from GH8 were used as an outgroup.

XynB(D646A) ΔNTD1 mutant can bind insoluble beechwood xylan separately. Such cases have been reported for other xylanases, such as Xyn30D (20) and Xyn10D (26). Notably, ratios and arrangement patterns between 1,4-linked β-D-xylopyranose and 1,3-linked β-D-xylopyranose residues and modifications of these xyloses of algal xylans differ greatly according to alga species and environmental conditions (27, 28), which are also different from those of the plant xylans used in this study. NTD1 of XynB may facilitate the hydrolysis of XynB on some algal xylans, which needs further study.

In addition to the N-terminal CBM (NTD1), our results show that the long NTD of XynB also contains two other functional regions, NTD2 (Y137 to A193) and NTD3 (L194 to T562). Although it is far away from the C-terminal catalytic domain in sequence, sequence alignment and structural modeling indicate that NTD2 contains an α-helix that is an essential structural element of the $(\alpha/\alpha)_6$ barrel of the catalytic domain of XynB. Biochemical analyses also support that NTD2 is essential for the activity of XynB. NTD3, which is next to the catalytic domain of XynB in sequence, was shown to be helpful in maintaining the thermostability of XynB. However, the NTD3 deletion increased the enzyme's activity at temperatures lower than 30°C and its activity and stability in 0 to 4 M NaCl. Thus, it seems that the presence of NTD3 does not facilitate the cold adaptation and salt tolerance of XynB. The mechanism involved needs to be studied further. Interruption of the catalytic domain by a noncatalytic large region has not yet been observed in other xylanases, indicating that XynB contains a new organization of the GH8 catalytic domain.

Endo-β-1,4-xylanases play a crucial role in natural xylan degradation and have been extensively used in industries such as food processing, animal feed, and kraft pulp biobleaching (29, 30). XynB is a modular endo-β-1,4-xylanase that contains a long NTD. Our functional analyses of the NTD of XynB indicate that XynB represents a kind of xylanase with a new domain architecture. Moreover, there is a class of bacterial xylanases from the sea with the same domain architecture as XynB. XynB and these homologs form a new group of GH8 xylanases. Because these xylanases are all from marine bacteria, their specific domain architecture may have significance for them to adapt to the marine environment, which needs further confirmation. Therefore, the results in this study will lead to a better understanding of marine xylanases.

TABLE 2 Primers used in this study

Gene product	Primer	Sequence (5′–3′)[a]
WT XynB	XynB-F	AAGAAGGAGATATACATATGGAAGTGAGCATTGATCACTTAAC
	XynB-R	TGGTGGTGGTGGTGCTCGAGTTCAGGCTCGTTTTCATTTGG
XynBΔNTD1	XynBΔNTD1-F	AAGAAGGAGATATACATATGTACCAGCAAAGCGGCAATGC
	XynB-R	TGGTGGTGGTGGTGCTCGAGTTCAGGCTCGTTTTCATTTGG
NTD1	NTD1-F	AAGAAGGAGATATACATATGGAAGTGAGCATTGATCACTTAACC
	NTD1-R	TGGTGGTGGTGGTGCTCGAGGTCGATAACCCAACTTAAGTCCTG
NTD2-NTD3	NTD2-NTD3-F	AAGAAGGAGATATACATATGTACCAGCAAAGCGGCAATGCC
	NTD2-NTD3-R	TGGTGGTGGTGGTGCTCGAGGCGAATATCGTTTGAATCAATCG
NTD3-CD	NTD3-CD-F	AAGAAGGAGATATACATATGCTACCGCAGCCCAGTAAAGG
	XynB-R	TGGTGGTGGTGGTGCTCGAGTTCAGGCTCGTTTTCATTTGG
CD	CD-F	AAGAAGGAGATATACATATGACAGTGCTGTATGGTGTGGGTG
	XynB-R	TGGTGGTGGTGGTGCTCGAGTTCAGGCTCGTTTTCATTTGG
NTD2-CD	NTD2-CD-F	CACCCACACCATACAGCACTGTAGCTTGGTCGGGCACCAATTCG
	NTD2-CD-R	CGAATTGGTGCCCGACCAAGCTACAGTGCTGTATGGTGTGGGTG
XynB(Y159A) ΔNTD1	Y159A-F	CGCTGCTTATCACACGGGTGAAGCTAAAAATTTCTTTGTTGAGCGT
	Y159A-R	ACGCTCAACAAAGAAATTTTTAGCTTCACCCGTGTGATAAGCAGCG
XynB(N161A) ΔNTD1	N161A-F	GCTTATCACACGGGTGAATATAAAGCTTTCTTTGTTGAGCGTGGCT
	N161A-R	AGCCACGCTCAACAAAGAAAGCTTTATATTCACCCGTGTGATAAGC
XynB(E165A) ΔNTD1	E165A-F	GAATATAAAAATTTCTTTGTTGCGCGTGGCTTAGCAACCCAAG
	E165A-R	CTTGGGTTGCTAAGCCACGCGCAACAAAGAAATTTTTATATTC
XynB(F186A) ΔNTD1	F186A-F	CCACCTATCAGCAATTGGCCGAATTGGTGCCCGACC
	F186A-R	GGTCGGGCACCAATTCGGCCAATTGCTGATAGGTGG
XynB(D646A)	XynB(D646A)-F	AAATACTCTTCGCCGGCTGGTGCAGGGTTGG
	XynB(D646A)-R	CCAACCCTGCACCAGCCGGCGAAGAGTATTT
XynB(D646A) ΔNTD1	XynB(D646A)-F	AAATACTCTTCGCCGGCTGGTGCAGGGTTGG
	XynB(D646A)-R	CCAACCCTGCACCAGCCGGCGAAGAGTATTT

[a]Sequences identical to that of vector pET22b are underlined.

MATERIALS AND METHODS

Materials and strains. *G. mesophila* KMM 241 was obtained from the DSMZ (DSM 15026[T]). *Escherichia coli* strains DH5α and BL21(DE3) were purchased from TransGen Biotech (China). Strain DH5α was used for gene cloning, and strain BL21(DE3) was used for gene expression. The vector pET22b (Novagen, USA) was used for the construction of expression plasmids. Insoluble beechwood xylan was purchased from Sigma (USA), and soluble wheat arabinoxylan (low viscosity) was obtained from Megazyme (Ireland). A bacterial genomic DNA extraction kit (Biotech, China) and a high-purity plasmid preparation kit (Biotech, China) were used for gene and plasmid preparation, respectively.

Truncation and site-directed mutagenesis. Using the genomic DNA of strain KMM 241 as the template, truncation mutations in *xynB* were generated by PCR amplification and cloned into the vector pET22b. Using the constructed plasmid pET22b-*xynB*Δ*NTD1* as the template, site-directed mutagenesis in *xynB*ΔNTD1 was performed with QuikChange mutagenesis kit II (Agilent Technologies, USA) according to a method of QuikChange site-directed mutagenesis reported previously (31), using primers containing mutations (Table 2). WT XynB and all mutants were expressed in *E. coli* BL21(DE3) cells, which were induced by the addition of 0.5 mM isopropyl-β-D-thiogalactopyranoside (IPTG) and cultured at 15°C for 24 h. Cells were collected and disrupted by sonication in 50 mM phosphate-buffered saline (PBS) (pH 7.0). The recombinant protein was first purified by using nickel-nitrilotriacetic acid resin (GE Healthcare, USA) and then purified by gel filtration chromatography on a Superdex 200 column (GE Healthcare, USA).

Enzyme assay and protein determination. Xylanase activity was measured as described previously by Guo et al., with insoluble beechwood xylan or soluble arabinoxylan as the substrate (11). The reaction mixture contained 0.01 ml of the enzyme and 0.09 ml of 30 mg/ml beechwood xylan or arabinoxylan dissolved in 50 mM PBS (pH 7.0). After incubation at 40°C for 10 min, the reaction was terminated by the addition of 0.15 ml of dinitrosalicylic acid (DNS) to the mixture. The amount of reducing sugar released into the mixture was determined with xylose as the standard, using the DNS method (32). One unit of enzyme activity was defined as the amount of enzyme required to liberate 1 μmol xylose per min. Enzyme kinetic assays were carried out with 50 mM PBS (pH 7.0) at 40°C, using arabinoxylan at

concentrations of 0 to 30.0 mg/ml. Kinetic parameters were calculated by nonlinear regression fit directly to the Michaelis-Menten equation using Origin8 software. The biochemical properties of XynB and its mutants were analyzed with arabinoxylan as the substrate. The optimal temperatures for the activities of WT XynB and its mutants XynBΔNTD1 and NTD2-CD were determined by incubating the reaction mixtures at temperatures ranging from 0 to 60°C. For the thermal stability assay, WT XynB and its mutants were preincubated at 35°C for different periods of time, and the residual activities were measured at 40°C. The effects of NaCl concentrations on the activities of WT XynB and its mutants were determined with 0 to 4 M NaCl. For salt tolerance assays, the enzyme was incubated at 4°C for 1 h in buffers containing NaCl at concentrations ranging from 0 to 4.0 M before the residual activity was measured at 40°C. The effects of pH on the activities of these three proteins were determined in the range of pH 4.0 to 10.0 at 40°C. The buffers used were 50 mM citrate buffer at pH 4.0 to 6.0, 50 mM PBS at pH 6.0 to 8.0, 50 mM Tris-HCl buffer at pH 8.0 to 9.0, and 50 mM glycine-NaOH buffer at pH 9.0 to 10.0. To determine the effect of pH on enzyme stability, the residual activities were measured after the enzymes were incubated in buffers with different pH values (pH 4.0 to 10.0) at 4°C for 1 h. The protein concentration was determined by using a Pierce bicinchoninic acid (BCA) protein assay kit (Thermo Scientific, USA) with bovine serum albumin (BSA; Sigma, USA) as the standard.

Adsorption assay. The abilities of WT XynB and its mutants to bind to insoluble beechwood xylan were assayed according to the method of Valenzuela et al. (20), with minor modifications. BSA served as the negative control. To avoid xylan hydrolysis in the assay of the xylan-binding abilities of XynB and XynBΔNTD1, two inactive mutants, XynB(D646A) and XynB(D646A) ΔNTD1, were constructed for use. Proteins were diluted to 0.1 mg/ml in 50 mM PBS (pH 7.0). The reaction mixture contained 20 mg of beechwood xylan and 200 μl of proteins. After incubation at 20°C at 180 rpm for 1 h, reaction mixtures were centrifuged at 13,000 rpm for 5 min, and the supernatants containing the unbound proteins were removed carefully. The resulting pellets were washed with 400 μl of 50 mM PBS (pH 7.0) three times. The pellets were then resuspended in 100 μl of 10% (wt/vol) SDS and boiled for 5 min to release the bound proteins. The total proteins (before adsorption), the unbound proteins in the supernatant, the proteins in the washing buffer, and the bound proteins in the pellet were analyzed by SDS-PAGE. The densitometric values of bands were determined by using Quantity One v4.6.2.

Circular dichroism spectroscopy. Circular dichroism spectra of XynBΔNTD1 and its mutants were recorded at 20°C on a J-810 spectropolarimeter (Jasco, Japan). All spectra were collected from 200 nm to 250 nm at a scanning rate of 200 nm/min with a path length of 0.1 cm. Concentrations of all proteins for circular dichroism spectroscopy assays were 0.3 mg/ml in 50 mM PBS (pH 7.0).

Homology modeling and sequence analysis. The homology model of mutant NTD2-CD was constructed by using SWISS-MODEL (33) with the crystal structure of BhRex (PDB accession number 1WU4) or PhXyl (PDB accession number 1H13) as the template, and all structure images were produced by using PyMOL software. Multiple-sequence alignment was carried out by using ClustalX (34). Secondary structures of XynB homologs with crystal structures were placed above/below the alignment by using ESPript (35). Phylogenetic analysis was performed by using MEGA6 (36).

SUPPLEMENTAL MATERIAL

Supplemental material for this article may be found at https://doi.org/10.1128/AEM.01785-18.

SUPPLEMENTAL FILE 1, PDF file, 1.3 MB.

ACKNOWLEDGMENTS

This work was supported by the National Natural Science Foundation of China (grants 41676180, 91751101, 31670063, and 31670038), the Qingdao National Laboratory for Marine Science and Technology (QNLM2016ORP0310), the AoShan Talents Cultivation Program supported by the Qingdao National Laboratory for Marine Science and Technology (2017ASTCP-OS14), and the Program of Shandong for Taishan Scholars (TS20090803).

We declare that we have no conflicts of interest with the contents of this article.

X.-L.C. and P.-Y.L. designed and directed the research. F.Z. and Y.-S.Y. performed the experiments. P.-Y.L., X.-L.C., and F.Z. wrote the manuscript. X.-Y.Z. and Y.-Z.Z. helped in analyzing data and revising the manuscript.

REFERENCES

1. Saha BC, Bothast RJ. 1999. Enzymology of xylan degradation. ACS Symp Ser 723:167–194. https://doi.org/10.1021/bk-1999-0723.ch011.
2. Henrissat B, Callebaut I, Fabrega S, Lehn P, Mornon JP, Davies G. 1995. Conserved catalytic machinery and the prediction of a common fold for several families of glycosyl hydrolases. Proc Natl Acad Sci U S A 92: 7090–7094. https://doi.org/10.1073/pnas.92.15.7090.
3. Gruber K, Klintschar G, Hayn M, Schlacher A, Steiner W, Kratky C. 1998. Thermophilic xylanase from *Thermomyces lanuginosus*: high-resolution X-ray structure and modeling studies. Biochemistry 37:13475–13485. https://doi.org/10.1021/bi980864l.
4. Yoon KH, Yun HN, Jung KH. 1998. Molecular cloning of a *Bacillus* sp. KK-1 xylanase gene and characterization of the gene product. Biochem Mol Biol Int 45:337–347.
5. Collins T, Meuwis MA, Stals I, Claeyssens M, Feller G, Gerday C. 2002.

A novel family 8 xylanase, functional and physicochemical characterization. J Biol Chem 277:35133–35139. https://doi.org/10.1074/jbc.M204517200.
6. Elleuche S, Piascheck H, Antranikian G. 2011. Fusion of the OsmC domain from esterase EstO confers thermolability to the cold-active xylanase Xyn8 from *Pseudoalteromonas arctica*. Extremophiles 15: 311–317. https://doi.org/10.1007/s00792-011-0361-8.
7. Lee CC, Kibblewhite-Accinelli RE, Wagschal K, Robertson GH, Wong DW. 2006. Cloning and characterization of a cold-active xylanase enzyme from an environmental DNA library. Extremophiles 10:295–300. https://doi.org/10.1007/s00792-005-0499-3.
8. Pollet A, Schoepe J, Dornez E, Strelkov SV, Delcour JA, Courtin CM. 2010. Functional analysis of glycoside hydrolase family 8 xylanases shows narrow but distinct substrate specificities and biotechnological potential. Appl Microbiol Biotechnol 87:2125–2135. https://doi.org/10.1007/s00253-010-2659-3.
9. Brennan Y, Callen WN, Christoffersen L, Dupree P, Goubet F, Healey S, Hernandez M, Keller M, Li K, Palackal N, Sittenfeld A, Tamayo G, Wells S, Hazlewood GP, Mathur EJ, Short JM, Robertson DE, Steer BA. 2004. Unusual microbial xylanases from insect guts. Appl Environ Microbiol 70:3609–3617. https://doi.org/10.1128/AEM.70.6.3609-3617.2004.
10. Hong PY, Iakiviak M, Dodd D, Zhang M, Mackie RI, Cann I. 2014. Two new xylanases with different substrate specificities from the human gut bacterium *Bacteroides intestinalis* DSM 17393. Appl Environ Microbiol 80:2084–2093. https://doi.org/10.1128/AEM.03176-13.
11. Guo B, Li PY, Yue YS, Zhao HL, Dong S, Song XY, Sun CY, Zhang WX, Chen XL, Zhang XY, Zhou BC, Zhang YZ. 2013. Gene cloning, expression and characterization of a novel xylanase from the marine bacterium, *Glaciecola mesophila* KMM241. Mar Drugs 11:1173–1187. https://doi.org/10.3390/md11041173.
12. Van Petegem F, Collins T, Meuwis MA, Gerday C, Feller G, Van Beeumen J. 2003. The structure of a cold-adapted family 8 xylanase at 1.3 A resolution. Structural adaptations to cold and investigation of the active site. J Biol Chem 278:7531–7539. https://doi.org/10.1074/jbc.M206862200.
13. Collins T, De Vos D, Hoyoux A, Savvides SN, Gerday C, Van Beeumen J, Feller G. 2005. Study of the active site residues of a glycoside hydrolase family 8 xylanase. J Mol Biol 354:425–435. https://doi.org/10.1016/j.jmb.2005.09.064.
14. Lagaert S, Van Campenhout S, Pollet A, Bourgois TM, Delcour JA, Courtin CM, Volckaert G. 2007. Recombinant expression and characterization of a reducing-end xylose-releasing exo-oligoxylanase from *Bifidobacterium adolescentis*. Appl Environ Microbiol 73:5374–5377. https://doi.org/10.1128/AEM.00722-07.
15. Honda Y, Kitaoka M. 2004. A family 8 glycoside hydrolase from *Bacillus halodurans* C-125 (BH2105) is a reducing end xylose-releasing exo-oligoxylanase. J Biol Chem 279:55097–55103. https://doi.org/10.1074/jbc.M409832200.
16. Fushinobu S, Hidaka M, Honda Y, Wakagi T, Shoun H, Kitaoka M. 2005. Structural basis for the specificity of the reducing end xylose-releasing exo-oligoxylanase from *Bacillus halodurans* C-125. J Biol Chem 280: 17180–17186. https://doi.org/10.1074/jbc.M413693200.
17. Boraston AB, Bolam DN, Gilbert HJ, Davies GJ. 2004. Carbohydrate-binding modules: fine-tuning polysaccharide recognition. Biochem J 382:769–781. https://doi.org/10.1042/BJ20040892.
18. Lombard V, Golaconda Ramulu H, Drula E, Coutinho PM, Henrissat B. 2014. The carbohydrate-active enzymes database (CAZy) in 2013. Nucleic Acids Res 42:D490–D495. https://doi.org/10.1093/nar/gkt1178.
19. Okazaki F, Tamaru Y, Hashikawa S, Li YT, Araki T. 2002. Novel carbohydrate-binding module of beta-1,3-xylanase from a marine bacterium, *Alcaligenes* sp. strain XY-234. J Bacteriol 184:2399–2403. https://doi.org/10.1128/JB.184.9.2399-2403.2002.
20. Valenzuela SV, Diaz P, Pastor FI. 2012. Modular glucuronoxylan-specific xylanase with a family CBM35 carbohydrate-binding module. Appl Environ Microbiol 78:3923–3931. https://doi.org/10.1128/AEM.07932-11.
21. Kleine J, Liebl W. 2006. Comparative characterization of deletion derivatives of the modular xylanase XynA of *Thermotoga maritima*. Extremophiles 10:373–381. https://doi.org/10.1007/s00792-006-0509-0.
22. Carrard G, Koivula A, Soderlund H, Beguin P. 2000. Cellulose-binding domains promote hydrolysis of different sites on crystalline cellulose. Proc Natl Acad Sci U S A 97:10342–10347. https://doi.org/10.1073/pnas.160216697.
23. Fujimoto Z. 2013. Structure and function of carbohydrate-binding module families 13 and 42 of glycoside hydrolases, comprising a beta-trefoil fold. Biosci Biotechnol Biochem 77:1363–1371. https://doi.org/10.1271/bbb.130183.
24. Kuramochi K, Uchimura K, Kurata A, Kobayashi T, Hirose Y, Miura T, Kishimoto N, Usami R, Horikoshi K. 2016. A high-molecular-weight, alkaline, and thermostable beta-1,4-xylanase of a subseafloor *Microcella alkaliphila*. Extremophiles 20:471–478. https://doi.org/10.1007/s00792-016-0837-7.
25. Hoffmam ZB, Zanphorlin LM, Cota J, Diogo JA, Almeida GB, Damasio AR, Squina F, Murakami MT, Ruller R. 2016. Xylan-specific carbohydrate-binding module belonging to family 6 enhances the catalytic performance of a GH11 endo-xylanase. N Biotechnol 33:467–472. https://doi.org/10.1016/j.nbt.2016.02.006.
26. Sakka M, Higashi Y, Kimura T, Ratanakhanokchai K, Sakka K. 2011. Characterization of *Paenibacillus curdlanolyticus* B-6 Xyn10D, a xylanase that contains a family 3 carbohydrate-binding module. Appl Environ Microbiol 77:4260–4263. https://doi.org/10.1128/AEM.00226-11.
27. Viana AG, Noseda MD, Gonçalves AG, Duarte ME, Yokoya N, Maria MC, Cerezo AS. 2011. β-D-(1$\rightarrow$4),β-D-(1$\rightarrow$3) 'mixed linkage' xylans from red seaweeds of the order Nemaliales and Palmariales. Carbohydr Res 346: 1023–1028. https://doi.org/10.1016/j.carres.2011.03.013.
28. Usov AI, Zelinsky ND. 2013. Chemical structures of algal polysaccharides, p 23–86. *In* Dominguez H (ed), Functional ingredients from algae for foods & nutraceuticals. Elsevier, Cambridge, United Kingdom.
29. Shallom D, Shoham Y. 2003. Microbial hemicellulases. Curr Opin Microbiol 6:219–228. https://doi.org/10.1016/S1369-5274(03)00056-0.
30. Collins T, Gerday C, Feller G. 2005. Xylanases, xylanase families and extremophilic xylanases. FEMS Microbiol Rev 29:3–23. https://doi.org/10.1016/j.femsre.2004.06.005.
31. Liu H, Naismith JH. 2008. An efficient one-step site-directed deletion, insertion, single and multiple-site plasmid mutagenesis protocol. BMC Biotechnol 8:91. https://doi.org/10.1186/1472-6750-8-91.
32. Miller GL, Blum R, Glennon WE, Burton AL. 1960. Measurement of carboxymethylcellulase activity. Anal Biochem 1:127–132. https://doi.org/10.1016/0003-2697(60)90004-X.
33. Biasini M, Bienert S, Waterhouse A, Arnold K, Studer G, Schmidt T, Kiefer F, Gallo Cassarino T, Bertoni M, Bordoli L, Schwede T. 2014. SWISS-MODEL: modelling protein tertiary and quaternary structure using evolutionary information. Nucleic Acids Res 42:W252–W258. https://doi.org/10.1093/nar/gku340.
34. Larkin MA, Blackshields G, Brown NP, Chenna R, McGettigan PA, McWilliam H, Valentin F, Wallace IM, Wilm A, Lopez R, Thompson JD, Gibson TJ, Higgins DG. 2007. Clustal W and Clustal X version 2.0. Bioinformatics 23:2947–2948. https://doi.org/10.1093/bioinformatics/btm404.
35. Robert X, Gouet P. 2014. Deciphering key features in protein structures with the new ENDscript server. Nucleic Acids Res 42:W320–W324. https://doi.org/10.1093/nar/gku316.
36. Tamura K, Stecher G, Peterson D, Filipski A, Kumar S. 2013. MEGA6: Molecular Evolutionary Genetics Analysis version 6.0. Mol Biol Evol 30:2725–2729. https://doi.org/10.1093/molbev/mst197.